Demonstration of X-Ray Amplification in Transient Gain Nickel-like Palladium Scheme

J. Dunn, A. L. Osterheld, R. Shepherd, W. E. White, V. N. Shlyaptsev,* and R. E. Stewart
Lawrence Livermore National Laboratory, Livermore, California 94550
(Received 29 September 1997)

We report experimental results of x-ray amplification of spontaneous emission in a Ni-like transient collisional excitation scheme. The Ni-like plasma formation, ionization, and collisional excitation requires irradiation of a slab target by two laser pulses: a formation beam with 5 J energy of 800 ps duration and a pump beam of 5 J energy in 1.1 ps. A gain of 35 cm^{-1} and a gL product of 12.5 are measured on the $4d \rightarrow 4p$ $J = 0 \rightarrow 1$ transition for Ni-like Pd at 147 Å with an 8 mm line focus. The high efficiency of this scheme at "table-top" laser energies is a direct consequence of the nonstationary population inversion produced by the high intensity picosecond pulse. [S0031-9007(98)05697-X]

PACS numbers: 42.55.Vc, 32.30.Rj, 42.60.By, 52.50.Jm

There has been much progress recently in producing x-ray lasers for different schemes pumped by energy sources that can be described as "table top." Fast capillary discharges have been utilized to produce saturation, with $gL > 25$, in a collisional Ne-like Ar laser at 469 Å [1]. A 10 Hz Pd-like Xe x-ray laser scheme has been demonstrated with $gL \sim 11$ at 418 Å for 40 fs irradiation of a xenon gas cell using field induced tunneling ionization followed by collisional excitation [2]. A shorter wavelength transient collisional scheme has been verified recently by Nickles *et al.* [3] for the Ne-like Ti $3p \rightarrow 3s$ transition at 326 Å where a high gain of 19 cm^{-1} and a gL product of ~9.5 were measured. This scheme has been recently reported to work with a $gL > 14$ for Ti and at 255 Å on Ne-like Fe by Dunn *et al.* [4] and to achieve saturated output for Ti [5]. Lasing has also been reported with gL products ≤ 6 for an H-like C recombination scheme at 182 Å using higher pumping energies [6], and for a multiple pulse collisional excitation scheme at 204 Å for Ni-like Nb [7] and H-like Li Ly-α inversion at 135 Å [8]. Generally, there has been a trend for laser-driven schemes away from high energy and towards high peak power by using drivers in the femtosecond or picosecond range to develop high efficiency, high output, shorter wavelength x-ray lasers [2–6,8]. Previously, collisional excitation Ni-like x-ray lasers in high-Z ions have been shown for $3d^9 4d \rightarrow 3d^9 4p$ transitions using large energy laser drivers [9,10]. The advantages of the Ni-like collisional excitation x-ray laser scheme are numerous. The larger x-ray photon energy to excitation energy ratio compared to Ne-like ions substantially improves the efficiency. Being similar to the Ne-like closed shell approach it has the same characteristics of collisional excitation x-ray lasers, where amplification can be extended to long plasma lengths while still exhibiting exponential output to saturation, for example, at 140 Å for Ag [11] and 73 Å for Sm [12]. Besides, it has predictable level structure scaling to shorter wavelengths, 35 Å for Au [13]. However, the production of a high output short pulse heated transient collisional excitation Ni-like laser has not been realized to date.

In this Letter we report x-ray amplification of spontaneous emission in a transient collisional excitation (TCE) Ni-like Pd ($Z = 46$) scheme pumped with less than 10 J of laser energy from a "table-top laser." We observe gain in excess of 35 cm^{-1} and a gL product of ~12.5 for the $4d \rightarrow 4p$ $J = 0 \rightarrow 1$ transition at 147 Å for target lengths up to 8 mm. This represents the shortest wavelength table-top, high gain $gL > 10$ x-ray laser observed to date and demonstrates amplification on the Ni-like analog of the TCE scheme. It has the inherent robustness of collisional excitation x-ray lasers, where amplification can be extended to long plasma lengths, but with much higher gains. Using this scheme driven at energies less than 20 J, it should be possible to realize a high gain x-ray laser well below 100 Å by scaling the Ni-like ion sequence to higher atomic numbers.

Although there have been various methods proposed to make collisional x-ray lasers more efficient by using multiple pulses [14], prepulses [15], and long pulse short pulse combinations [16], these are still variations of the quasi-steady state (QSS) inversion scheme. A new approach has been described by Afanasiev and Shlyaptsev [17], where a large transient population inversion can be achieved on a time scale of femtoseconds to a few tens of picoseconds. This is characterized by the plasma lifetime dictated by the fast pumping source, which in turn should be comparable with the relaxation time scales of the excited levels. The TCE scheme differs from QSS in a number of areas, but mainly because the rise time of the level excitation rates is shorter than the collisional excitation time scales. This produces a short-lived transient population inversion pumped directly from the ground state until collisions redistribute populations among all levels finally achieving the QSS state. Since during the time of population redistribution the inversion is defined by the upper laser level population, it is predicted that TCE will produce very high gains above 100 cm^{-1} and, therefore, high efficiency x-ray lasers.

One way to realize a TCE x-ray laser experimentally requires two stages of laser irradiation [3]. A formation

pulse of 1 ns heats a solid planar target at 10^{12} W cm^{-2} to produce a long scale length plasma with a Ni-like ionization stage. Depending on the required initial temperature, degree of ionization, electron density, and density gradients, a delay is essential before the second pulse to optimize the conditions within the plasma for maximum amplification. The short 1 ps pump pulse at 10^{15} W cm^{-2} produces efficient, rapid plasma heating with an increase in the electron temperature $T_e \geq \Delta E_u$, where $\Delta E_u = 450.3$ eV is the upper laser level excitation energy. This generates the transient inversion. The high gain conditions will last for a few picoseconds and will quickly decay after 5 to 15 ps as a result of collisional redistribution of the electron population among all excited levels, ionization, and plasma cooling. Therefore, high gain on short 1–3 mm lengths is expected: The gain will decrease for longer lengths since the x-ray laser transit time along the line focus exceeds the characteristic transient gain time scale.

The experiments were performed at the Lawrence Livermore National Laboratory Janus laser facilities. An 800 ps (FWHM) pulse at 1064 nm wavelength with 5–6 J on target produced the long scale length plasma by using one arm of the Janus laser. Since only the laser rod amplifiers were fired, a repetition rate of 1 shot every 3 minutes was possible. The short pulse beam was produced by the 5–6 J hybrid chirped pulse amplification Janus 500 fs system based on a Ti:sapphire oscillator and regenerative amplifier front end tuned to 1053 nm wavelength with Nd:phosphate glass power amplifiers described elsewhere [18]. This laser occupies two standard optical tables of dimensions 1.2×3.6 m with total area less than 10 m^2. The pulse duration was lengthened to 1.1 ps by detuning the compressor gratings. The regenerative amplifiers of the two lasers were synchronized using the 80 MHz radio-frequency output from the short pulse oscillator resulting in a relative timing jitter of 80 ps rms. The arrival of the short pulse was delayed by 1–2 ns relative to the peak of the long pulse to minimize refraction effects from plasma density gradients. Laser parameters including energy, temporal shapes, and synchronization, near field image, focal spot and spectrum were monitored on every shot. The two beams were aligned and copropagated under vacuum to the target chamber. The line focus of 70 μm $\times$ 12.5 mm was generated by the combination of a cylindrical lens and a paraboloid. Planar slab palladium targets were first aligned normal to the laser axis at installation and rotated back 10 to 25 mrad to compensate for plasma refraction of the x-ray laser output. The main diagnostic, aligned to the axis of the line focus, was a 1200 lines/mm flat-field grating spectrometer with a back-thinned 1024×1024 charge-coupled device (CCD) compact camera [19] to cover 130–350 Å. A gold-coated cylindrical mirror collection optic imaged the plasma gain region with 1:1 magnification onto a 100 μm wide entrance slit. The effective angular field of view which was integrated over in our geometry was 28×20 mrad in the horizontal and vertical directions, respectively. Additional instruments included a CCD x-ray slit camera with 25 μm spatial resolution to monitor line focus uniformity.

Figure 1 shows the strong $4d \rightarrow 4p$ $J = 0 \rightarrow 1$ transition at 147 Å observed in second order from the axial spectrum of an 8 mm long Pd slab. We have a measured uncertainty of ± 1 Å on this transition which is in good agreement with the predicted 148 Å wavelength [20]. Laser driver energies were 4.2 J in 800 ps at a peak intensity of 0.7 TW cm^{-2} and 5.2 J in 1.1 ps at 700 TW cm^{-2} on target with the short pulse delayed by 1.34 ns relative to the peak of the long pulse. This corresponds to a linear fluence of only 340 and 420 mJ/linear mm in the long and short pulse, respectively. The small edge structure observed at 123 Å in second order is identified as the Si L edge from absorption layers on the surface of the back-thinned CCD.

Very large increases in the laser output were observed at the shortest target lengths and required 0.5 and 1 mm increments. This is illustrated in Fig. 2 where the axial spectrum is shown for 1.03, 2.0, and 3.01 mm long Pd slabs. The x-ray laser transition is weak but visible for 1 mm lengths [4]. It is unambiguously identified at this target length on several counts: Variations in the x-ray laser intensity are observed as a function of short pulse laser energy, and differences in the vertical divergence are noted in comparison to the adjacent nonamplified lines. By increasing the target length in steps of 0.5 mm, strong exponentiating behavior is observed. The 2 mm spectrum exhibits more than 1 order of magnitude higher x-ray laser output and similar increases are measured for the 3 mm target length where the x-ray laser line begins to dominate the spectrum.

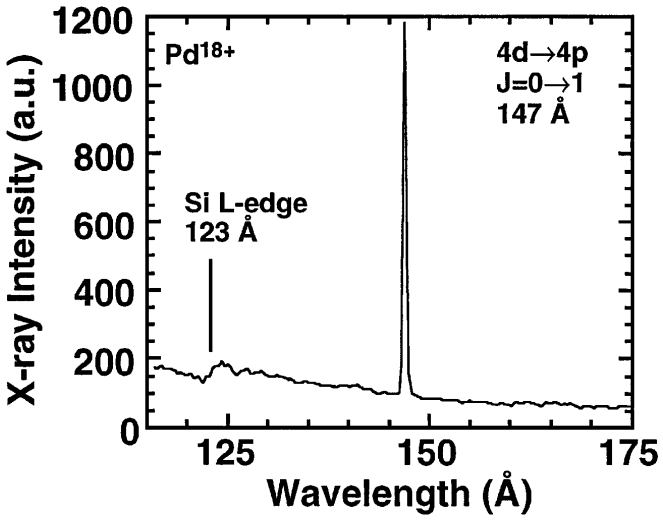

FIG. 1. Spectrum from 8 mm long Pd target showing strong Ni-like Pd $4d \rightarrow 4p$ $J = 0 \rightarrow 1$ x-ray laser transition at 147 Å measured in second order. Laser driven energies on target were 4.2 J in 800 ps and 5.2 J in 1.1 ps.

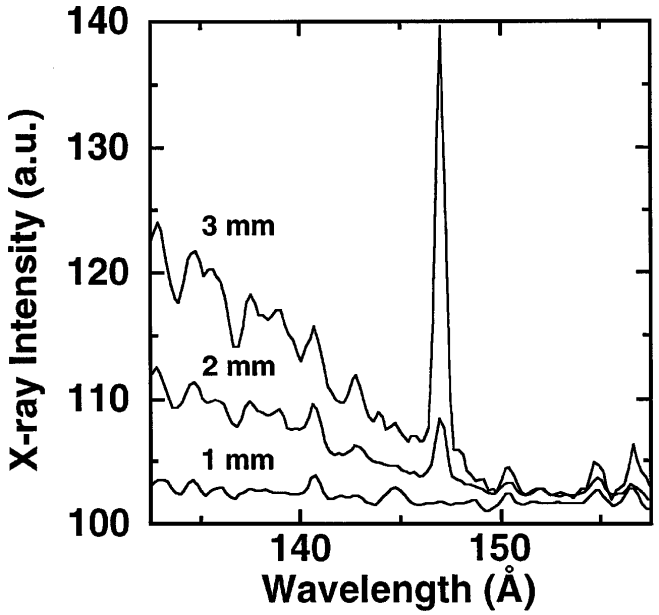

FIG. 2. Spectrum from target lengths of approximately 1, 2, and 3 mm of Pd showing Ni-like Pd $4d \rightarrow 4p$ $J = 0 \rightarrow 1$ x-ray laser line at 147 Å in second order. The transition is weak but visible for 1 mm target. The intensity increases by more than 2 orders of magnitude for 3 mm length.

We performed a careful characterization of the x-ray laser output, shown in Fig. 3, from 1 mm to a maximum of 8 mm Pd lengths in order to understand the transient gain behavior. The continuous line is a guide through the data points. The error bars in the measured x-ray laser intensity at short target lengths are mainly as a result of blending with an adjacent line. Laser shots were selected to give constant conditions for the length scan by holding parameters, including the relative delay and the driver energy constant to $\pm 6\%$. For 8 mm target lengths we observe the x-ray laser output to be reproducible to $\pm 40\%$. We measure an increase of 4 orders of magnitude in intensity for up to 8 mm. More than 1 order of magnitude increase is observed between 1 and 2 mm, which indicates the largest gain with values of 35.3 cm^{-1}, using the Linford equation fitted to the averaged data points [21]. Within error bars, the maximum gain for up to 1.5 mm length could be as high as 46 cm^{-1}. The intensity and gain smoothly decrease with increasing target length exhibiting an effect similar to saturation. However, this is, in fact, due mainly to transit time effects where the x-ray laser experiences gradually decreasing gain during propagation. There are also partial contributions from refraction effects and a shift of the optimum amplification region to higher densities for shorter target lengths [3]. The gain is measured to be 20 cm^{-1} for 2.5 mm, 11 cm^{-1} for 4 mm, 7 cm^{-1} for 6 mm lengths, and falling to 3.9 cm^{-1} for above 7 mm lengths. The overall gain length product $gL \sim 12.5 \pm 0.5$ is determined by continuously calculating the gain with length and integrating over the full 8 mm target length.

Gains in excess of 300 cm^{-1} have been predicted for transient gain in Ni-like Xe at 96 Å [17] and recently for a Ni-like Mo 189 Å laser [22] at irradiances and laser pulse durations close to this work. Similarly high values were also calculated for Ne-like schemes [17,23]. Our observations indicate that the gain region occurs further out at 50–100 μm from the target surface and, therefore, at a lower plasma density than described, for example, in [22]. The gain measurements here, although significantly

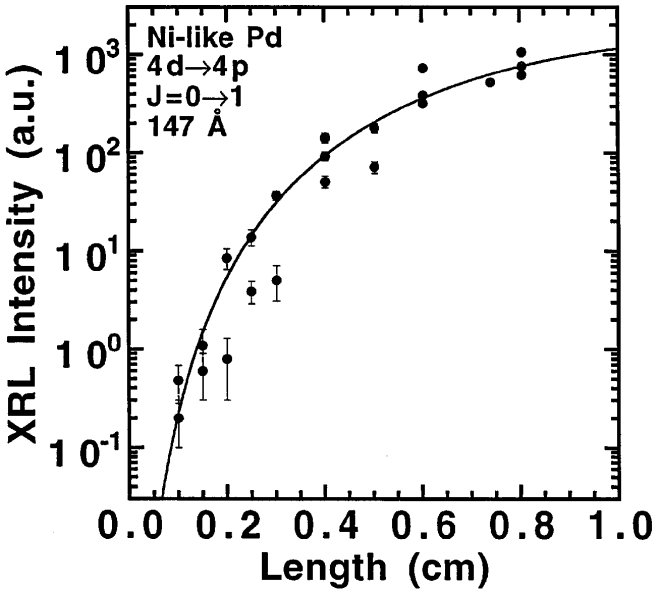

FIG. 3. Intensity of 147 Å x-ray laser line, measured in second order, for 1 to 8 mm Pd target lengths. Continuous line is a guide through the experimental points indicating changing transient gain as the x-ray laser propagates along the plasma column.

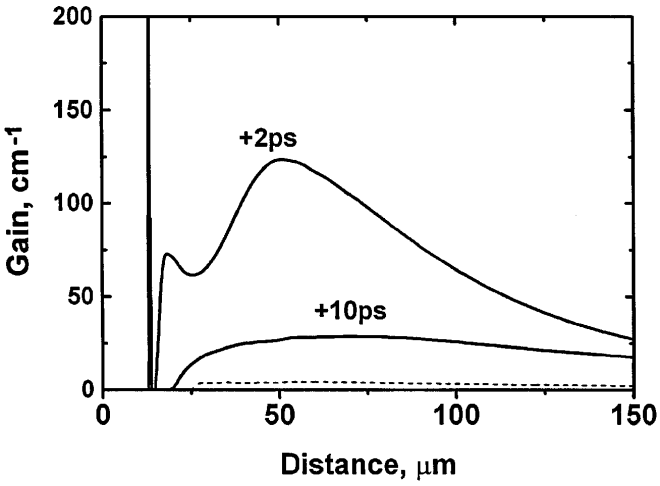

FIG. 4. Transient $J = 0 \rightarrow 1$ gain profiles as calculated by the code RADEX at 2 ps (+2 ps curve) and 10 ps (+10 ps curve) after arrival of 1 ps laser pulse. For comparison, the QSS gain is shown at 2 ps (dashed curve).

higher than most x-ray laser results reported to date, fall short of these predicted values. The main reasons for the difference can be explained by several effects including refraction, reduced effective amplification path due to short gain lifetime, and collisional line broadening [3]. For the modeling of our experimental conditions we used the one-dimensional numerical code RADEX [3,17], which treats the transient hydrodynamics, atomic kinetics, and radiation transport self-consistently with an additional ray-tracing package to calculate the x-ray laser intensity. The transient $J = 0 \rightarrow 1$ gain, shown in Fig. 4, is very inhomogeneous in space and time reaching high values of 200 cm^{-1} during the first 2 ps after the short pulse ($+2$ ps curve) and decreases rapidly to 28 cm^{-1} by 10 ps ($+10$ ps curve). The former occur near the critical density in the thin, steep ablative layer (isolated spike at 15 μm in Fig. 4) while the latter are in areas of relatively flat, lower density profile 30–100 μm from the target surface. Refraction, caused by density gradients normal to the target surface, deflects the x-ray laser out of the high density and high gain region within 25 μm from the target surface as it propagates along the plasma column. For comparison, the QSS gain (dashed curve) of ~ 4 cm^{-1} at 2 ps is substantially lower than the transient gain. Second, the conjunction of the fast transient nature of the atomic kinetics and the long photon transit time L/c are significant. The short inversion lifetime near the high density critical region decreases the photon effective amplification path in the high gain region to an axial length of 500 μm. As a consequence of all these effects, the gain-length product is substantially decreased in the high density plume. The peripheral plasma regions at lower density $n_e \sim (0.9\text{–}2) \times 10^{20}$ cm^{-3} with smaller local gains and with longer inversion lifetimes are more optimal for amplification resulting in larger local gL. Further improvement in the gain and efficiency is possible by using a prepulse or low density target and traveling wave irradiation [17].

In conclusion, we have demonstrated x-ray amplification in Ni-like transient collisional excitation scheme at 147 Å. This has resulted in the shortest wavelength high transient gain x-ray laser demonstrated to date using table-top laser energies. Gains of 35 cm^{-1} have been measured with gL product of ~ 12.5 at a repetition rate of 1 shot/3 minutes. It should be possible to improve the efficiency and extrapolate to shorter wavelengths with the Ni-like ion isoelectronic sequence by implementing traveling wave geometry irradiation on high-Z targets [24,25].

The continued support of M. Eckart is greatly appreciated. We acknowledge the technical contributions from J. Hunter, B. Sellick, D. Swan, and A. Ellis. We thank J. Nilsen for comments made on the manuscript. One of us (V. N. S.) acknowledges support from H. Baldis of ILSA and Yu. Afanasiev of LPI. This work was performed under the auspices of the U.S. Department of Energy by the Lawrence Livermore National Laboratory under Contract No. W-7405-Eng-48.

*Permanent address: P. N. Lebedev Physical Institute, Leninsky Prospect 53, Moscow Russia.

[1] J. J. Rocca *et al.,* Phys. Rev. Lett. **73**, 2192 (1994); Phys. Rev. Lett. **77**, 1476 (1996).
[2] B. E. Lemoff *et al.,* Phys. Rev. Lett. **74**, 1574 (1995).
[3] P. V. Nickles *et al.,* Proc. SPIE Int. Soc. Opt. Eng. **2520**, 373 (1995); Phys. Rev. Lett. **78**, 2748 (1997).
[4] J. Dunn *et al.,* Proc. SPIE Int. Soc. Opt. Eng. **3156**, 114 (1997).
[5] P. V. Nickles *et al.,* Proc. SPIE Int. Soc. Opt. Eng. **3156**, 80 (1997).
[6] J. Zhang *et al.,* Phys. Rev. Lett. **74**, 1335 (1995).
[7] S. Basu *et al.,* Appl. Phys. B **57**, 303 (1993).
[8] D. V. Korobkin *et al.,* Phys. Rev. Lett. **77**, 5206 (1996).
[9] B. J. MacGowan *et al.,* Phys. Rev. Lett. **59**, 2157 (1987).
[10] S. Maxon *et al.,* Phys. Rev. A **37**, 2227 (1988).
[11] J. Zhang *et al.,* Phys. Rev. Lett. **78**, 3856 (1997).
[12] J. Zhang *et al.,* Science **276**, 1097 (1997).
[13] B. J. MacGowan *et al.,* Phys. Fluids B **4**, 2326 (1992).
[14] L. B. Da Silva *et al.,* Opt. Lett. **19**, 1532 (1994); J. C. Moreno *et al.,* Opt. Commun. **110**, 585 (1994).
[15] T. Boehly *et al.,* Phys. Rev. A **42**, 6962 (1990); J. Nilsen *et al.,* Phys. Rev. A **48**, 4682 (1993).
[16] L. B. Da Silva *et al.,* Proc. SPIE Int. Soc. Opt. Eng. **1229**, 128 (1990); S. Maxon *et al.,* Phys. Rev. Lett. **70**, 2285 (1993).
[17] Yu. V. Afanasiev and V. N. Shlyaptsev, Sov. J. Quantum Electron. **19**, 1606 (1989); V. N. Shlyaptsev *et al.,* Proc. SPIE Int. Soc. Opt. Eng. **2012**, 111 (1993).
[18] J. Dunn *et al.,* in *Proceedings of the 12th International Conference on Laser Interaction and Related Plasma Phenomena,* edited by S. Nakai and G. H. Miley, AIP Conf. Proc. No. 369 (AIP, New York, 1996), p. 652.
[19] A. D. Conder *et al.,* Rev. Sci. Instrum. **66**, 709 (1995); J. Dunn *et al.,* Proc. SPIE Int. Soc. Opt. Eng. **2654**, 119 (1996).
[20] J. H. Scofield and B. J. MacGowan, Phys. Scr. **46**, 361 (1992).
[21] G. J. Linford, E. R. Peressini, W. R. Sooy, and M. L. Spaeth, Appl. Opt. **13**, 379 (1974).
[22] J. Nilsen, J. Opt. Soc. Am. B **14**, 1511 (1997).
[23] K. G. Whitney *et al.,* Phys. Rev. E **50**, 468 (1994); S. B. Healy *et al.,* Opt. Commun. **132**, 442 (1996); J. Nilsen, Phys. Rev. A **55**, 3271 (1997).
[24] G. J. Tallents, University of Essex, Colchester CO4 3SQ, UK (private communication).
[25] Since these results, a long pulse amplifier has been built on the picosecond laser optical tables to produce a multiple pulse x-ray laser driver system.